Transcriptomics reveal stretched human pluripotent stem cell-derived cardiomyocytes as an advantageous hypertrophy model

Lotta Pohjolainen[1], Heikki Ruskoaho[1], Virpi Talman[1]

[1]Drug Research Program and Division of Pharmacology and Pharmacotherapy, Faculty of Pharmacy, University of Helsinki, FI-00014 Helsinki, Finland

Correspondence: Virpi Talman, Ph.D., Division of Pharmacology and Pharmacotherapy, Faculty of Pharmacy, University of Helsinki, PO Box 56, FI-00014 Helsinki, Finland. E-mail: virpi.talman@helsinki.fi. ORCID: 0000-0002-2702-6505

Keywords: Cardiomyocytes; Induced Pluripotent Stem Cells; Gene Expression; Transcriptomics; Left Ventricular Hypertrophy

Summary statement

Distinct hypertrophic gene expression changes in mechanically stretched human induced pluripotent stem cell-derived cardiomyocytes reveal the utility of these cells as an advantageous *in vitro* model for mechanical overload-induced hypertrophy.

Abstract

Left ventricular hypertrophy, characterized by hypertrophy of individual cardiomyocytes, is an adaptive response to an increased cardiac workload that eventually leads to heart failure. Previous studies using neonatal rat ventricular myocytes (NRVMs) and animal models have revealed several hypertrophy- and mechanical load-associated genes and signaling pathways. However, these models are not directly applicable to humans. Here, we studied the effect of cyclic mechanical stretch on gene expression of human induced pluripotent stem cell-derived cardiomyocytes (hiPSC-CMs) using RNA sequencing. HiPSC-CMs showed distinct hypertrophic changes in gene expression at the level of individual genes and in biological processes. We also identified several differentially expressed genes that have not been previously associated with cardiomyocyte hypertrophy and thus serve as attractive targets for future studies. When compared to previously published data attained from stretched NRVMs and human embryonic stem cell-derived cardiomyocytes, hiPSC-CMs displayed a smaller number of changes in gene expression, but the differentially expressed genes revealed more pronounced enrichment of hypertrophy-related biological processes and pathways. Overall, these results establish hiPSC-CMs as a valuable in vitro model for studying human cardiomyocyte hypertrophy.

Introduction

The prevalence of cardiovascular diseases, including coronary artery disease and hypertension, is increasing rapidly, from approximately 271 million in 1990 to 523 million in 2019 (University of Washington, Institute of Health Metrics and Evaluation, 2021). However, treatment strategies have not evolved correspondingly; hence, cardiovascular disease is the leading cause of death (Roth et al., 2017). Hypertension and myocardial infarction increase cardiac workload, causing structural and functional changes in the myocardium (Frey et al., 2004). These changes include left ventricular hypertrophy, which is characterized by cardiomyocyte enlargement. Although it is initially an adaptive response to physiological and pathological stimuli, such as mechanical stretch or neurohumoral activation, prolonged hypertrophy leads to contractile dysfunction and heart failure.

In response to hypertrophic stimuli, cardiomyocytes not only increase in size but also increase their protein synthesis, sarcomeres become disorganized, and specific changes in gene expression occur

(Lorell and Carabello, 2000). The early genetic response to stretch is activation of immediate early response genes, such as proto-oncogenes *FOS* and *JUN*, components of the transcription factor AP-1. This is followed by upregulation of natriuretic peptide B (BNP) coding gene (*NPPB*) and reactivation of fetal genes such as natriuretic peptide A (*NPPA*), myosin-7 (*MYH7*), and skeletal muscle α-actin (*ACTA1*). A variety of effectors and signaling pathways mediate the hypertrophic response (Heineke and Molkentin, 2006). For example, studies in animal models and in neonatal rat ventricular myocytes (NRVMs) have identified mitogen-activated protein kinase (MAPK) (Rose et al., 2010), protein kinase C (PKC) (Palaniyandi et al., 2009) and bromodomain and extraterminal domain (BET) proteins (Borck et al., 2020) as potential mediators transducing the hypertrophic response in cardiomyocytes. However, controversial results of the exact role of these signal transducers have also been published, which can partially be explained by the use of different experimental models.

Cardiomyocyte hypertrophy has commonly been studied in animal models *in vivo* or in isolated NRVMs *in vitro* (Heineke and Molkentin, 2006). However, studies conducted with animals or animal cells are not always directly translatable to humans. Human induced pluripotent stem cell-derived cardiomyocytes (hiPSC-CMs) offer a unique possibility to investigate human cardiomyocytes and abolish the effects of species differences. However, although hiPSC-CMs beat spontaneously, they are relatively immature by structural, metabolic and electrophysiological properties (Robertson et al., 2013; Földes et al., 2014). We and others have previously shown that hiPSC-CMs respond to endothelin-1 (ET-1) by increasing the expression of pro-B-type natriuretic peptide (proBNP) and the corresponding gene (*NPPB*) along with other hypertrophy-related genes, although no morphological change was observed (Pohjolainen et al., 2020; Carlson et al., 2013). On the other hand, Földes et al. (Földes et al., 2014) showed that hiPSC-CMs lack the hypertrophic response to α-adrenergic stimuli. Hence, it seems that not all hypertrophic signaling pathways are functional in hiPSC-CMs.

The aim of this study was to characterize the transcriptomic response of hiPSC-CMs to mechanical stretch. In addition, we compared stretch-induced gene expression changes to previously published data from stretched NRVMs and human embryonic stem cell-derived cardiomyocytes (hESC-CMs) (Rysä et al., 2018; Ovchinnikova et al., 2018). We also used our model to test the involvement of different signaling pathways in mechanical load-induced hypertrophy of hiPSC-CMs by pharmacological inhibition of several signaling molecules.

Results

Mechanical stretch induces natriuretic peptide gene expression in hiPSC-CMs

The mechanical stretch model of hiPSC-CMs was first validated by measuring the mRNA expression of *NPPA* and *NPPB*, hallmark genes of cardiomyocyte hypertrophy (Ogawa et al., 1995). After 24 h of

cyclic mechanical stretch, hiPSC-CMs showed increased expression of both *NPPA* and *NPPB* (Fig. 1A,B). At 48 h and 72 h, the upregulation of the *NPPA* and *NPPB* mRNA levels was not statistically significant, although increased gene expression was observed in each independent experiment.

Mechanical stretch-induced genome-wide gene expression program in hiPSC-CMs

To identify genome-wide gene expression changes regulated by mechanical stretch, we performed RNA sequencing (RNAseq) at 24 h, 48 h and 72 h of mechanically stretched hiPSC-CMs and their unstretched controls. Principal component analysis showed strong separation of stretched and control samples at 24 h and 48 h defined by two principal components (Fig. S1). However, after 72 h of stretching, no clear difference between stretched and unstretched groups was detected, while separation of individual experiments was seen instead. These findings suggest strong conserved early responses to stretch and increased biological variation over time.

Of the 30,861 genes identified in our samples, 134 genes showed differential expression (FC>1.5, false discovery rate (FDR)-adjusted $p<0.05$) after stretching. Our analysis identified 75, 28 and 2 upregulated genes in response to 24 h, 48 h and 72 h of stretch, respectively (Fig. 1C). In addition, 12, 30 and 0 genes were downregulated in response to 24 h, 48 h and 72 h of stretch, respectively (Fig. 1D). Venn diagrams demonstrated minor overlaps between time points, indicating time-dependent regulation of gene expression. The top 12 differentially expressed genes at each time point are presented in Fig. 1E,F. The full data are available in Dataset S1.

Multiple hypertrophy-associated genes were upregulated. These include fetal genes coding for natriuretic peptides (*NPPA* and *NPPB*), skeletal alpha actin 1 (*ACTA1*), and transgelin (*TAGLN*), and several genes encoding contractile proteins, such as cardiac alpha actin (*ACTC1*), myosin light chain 3 (*MYL3*), troponins (*TNNI3*, *TNNC1*), and tropomyosin 2 (*TPM2)*. In addition to contractile proteins, other cytoskeletal proteins, such as alpha- and beta-tubulins (*TUBA4A*, *TUBA1A*, *TUBB2A*, *TUBB6*), alpha-actinin 1 (*ACTN1)*, nestin (*NES*) and keratins (*KRT8*, *KRT18*), were upregulated. These changes confirm that mechanical stretching of hiPSC-CMs induces alterations in gene expression, which are characteristic for cardiomyocyte hypertrophy. The upregulated genes mainly encode enzymes (26), exosomal proteins (20) and cytoskeletal proteins (15), while the downregulated genes encode enzymes (6) and transcription factors (6) (Table S2).

We chose eleven genes for validation by qRT-PCR. The selection was first based on differential expression of both up- and downregulated genes. Second, both protein-coding and noncoding (*LINC00648*, *PTPRG-AS1*) genes were chosen. In addition, different protein-coding genes were selected, including hypertrophy-associated secreted peptides (*NPPA*, *NPPB*), cytoskeletal proteins (*ACTA1*, *ACTC1*, *ACTN1*, *TNNI3*), a transcription factor (*CSRP3*) and a transporter protein

(*SLC16A9*). Overall, similar results were obtained with both qRT-PCR and RNAseq (Fig. 2), except for *ACTN1*, which showed downregulation in qRT-PCR and slight upregulation in RNAseq after 72 h of stretch (Fig. 2A).

Comparison of differentially expressed genes in hiPSC-CMs, NRVMs and hESC-CMs

We compared our data with the NRVM data published by Rysä et al. (Rysä et al., 2018) to elucidate similarities and differences between these two *in vitro* cardiomyocyte models from different species. Both we and Rysä et al. (Rysä et al., 2018) used time points of 24 h and 48 h; hence, these were chosen for comparison, although the equivalency of these time points between species has not been proven. Overall, the number of differentially expressed genes was drastically different; for example, after a 48-h stretch, over 600 genes were upregulated in NRVMs, while only 28 genes were upregulated in hiPSC-CMs (Fig. 3). Interestingly, 21 differentially expressed genes showed similar changes in both cell models. In fact, 3 genes were upregulated in both cardiomyocyte types at both time points: *CASQ1*, *TIMP1* and *TUBB2B*. We did not identify genes that were consistently downregulated in both CM types at 24h and 48 h. Comparison of cell types after 24 h of stretch showed that 14 genes were upregulated in both cell types, while no commonly downregulated genes were identified (Fig. 3C). After 48 h of stretch, 8 genes were upregulated, and 2 genes were downregulated in both cell types (Fig. 3D). Cross comparison of different time points revealed 5 upregulated genes and 2 downregulated genes in hiPSC-CMs after 48 h of stretch and in NRVMs after 24 h of stretch (Table S3). In addition, 20 upregulated genes and one downregulated gene in hiPSC-CMs after a 24-h stretch were similarly differentially expressed in NRVMs after a 48-h stretch. Hence, the differentially expressed genes showed the most similarity between upregulated genes in hiPSC-CM at 24 h and in NRVMs at 48 h. Only three genes showed opposing expression in hiPSC-CMs and NRVMs: *MASP1*, *ENO3*, and *CES1* were upregulated in hiPSC-CMs but downregulated in NRVMs.

We also compared our differential gene expression data at 48 h with that from 48 h stretched hESC-CMs reported by Ovchinnikova et al. (Ovchinnikova et al., 2018). Of 936 differentially expressed genes in stretched hESC-CMs, only 13 genes were similarly expressed in hiPSC-CMs: four genes were upregulated, and nine genes were downregulated. The upregulated genes included *TUBB2B*, which was upregulated in all cell types (hiPSC-CMs, NRVMs and hESC-CMs) after 24 h (not studied in hESC-CMs) and 48 h of stretching. Other upregulated genes were *DUSP13*, *ACAT2* and *ENO3*. In addition, one of the genes downregulated in both hiPSC-CMs and NRVMs, *ZNF519*, was also downregulated in hESC-CMs. In hiPSC-CMs and hESC-CMs, no changes in opposite directions were observed in any differentially expressed gene. All common differentially expressed genes and their fold changes are presented in Table S3.

Functional analysis of differentially expressed genes in stretched hiPSC-CMs

To identify the biological functions regulated by the differentially expressed genes, we performed Gene Ontology (GO) enrichment analysis. The GOrilla analysis recognized 18,992 genes out of 30,861 gene terms entered. Only 15,554 of these genes were associated with a GO term, and these were used for enrichment calculation. Enriched GO terms were found only for upregulated genes. The enriched biological processes of upregulated genes at all time points are presented in Figs. 4A and S2. All enriched processes were highly related to cardiomyocyte hypertrophy. Actin filament-based movement, more specifically actin-myosin filament sliding and muscle filament sliding, was the most enriched biological process. Other enriched processes can be grouped under four categories: muscle contraction, secretion, regulation of cell death, and steroid biosynthesis. This result indicates that very specific biological processes are activated in hiPSC-CMs in response to stretching.

We also searched for enriched GO terms for molecular function and cellular components. Again, enriched GO terms were only found for upregulated genes. Three molecular functions were significantly overrepresented: structural molecule activity, structural constituent of the cytoskeleton, and calcium-dependent protein binding (Fig. S3A). Among the cellular components, 14 GO terms, especially terms related to extracellular vesicles, supramolecular complexes and cytoskeleton, were enriched (Fig. S3B). These analyses confirm that structural and cytoskeletal protein-coding genes are among the most upregulated genes in stretched hiPSC-CMs. The complete data of the GO analyses are available in Dataset S2.

Comparison of the functional analysis of hiPSC-CMs and NRVMs

To compare stretch-induced enriched biological processes of hiPSC-CMs and NRVMs, we performed a similar GO analysis for upregulated genes of NRVMs studied by Rysä et al. (Rysä et al., 2018). In line with a higher number of upregulated genes in NRVMs compared to hiPSC-CMs, more enriched biological processes were found (71 GO terms). Hence, while a very limited number of specific processes were enriched in stretched hiPSC-CMs, a broad range of biological processes were detected in NRVMs. The most evidently enriched biological processes associated with upregulated genes in NRVMs were RNA metabolic processes, response to stimulus, biosynthetic processes, cellular component biogenesis, developmental processes, and regulation of cell death (Fig. 4B). Upregulated genes from both hiPSC-CMs and NRVMs thus share GO terms associated with the regulation of apoptosis and steroid biosynthesis.

To further discover the functionality of the differentially expressed genes, KEGG and Reactome pathway analyses were performed. KEGG pathway analysis revealed 11 and 10 enriched pathways in upregulated genes in hiPSC-CMs and NRVMs, respectively (Fig. 5A,B). However, none of the

pathways was common to both cell types. In hiPSC-CM, the pathways included cardiac- and cardiomyocyte-associated pathways, while the enriched terms in NRVMs were heterogeneous, and half of them were cancer-associated. In turn, Reactome pathway analysis resulted in 31 and 17 enriched pathways for hiPSC-CMs and NRVMs, respectively (Fig. 5C,D). Three pathways were enriched in both cell types: striated muscle contraction, HSP90 chaperone cycle for steroid hormone receptors (SHRs), and the role of GTSE1 in G2/M progression after theG2 checkpoint.

Enriched transcription factor targets of stretch-induced genes

Several transcription factors (TFs) are associated with cardiomyocyte hypertrophy (Heineke and Molkentin, 2006; Kohli et al., 2011). Hence, we analyzed which TF target sites were enriched in response to stretch. In our analysis, 19 and 18 TF binding sites were enriched in upregulated genes of stretched hiPSC-CMs and NRVMs, respectively (Fig. 6A,B). Most of the enriched binding sites were for serum response factor (SRF), which had 5 enriched binding sites in both cell types. SRF controls the expression of genes regulating the cytoskeleton during development and cardiac hypertrophy (Coletti et al., 2016; Nelson et al., 2005). In addition, two binding sites for the transcription factor c-Jun, which is part of the AP-1 complex and is involved in cardiomyocyte hypertrophy and increased steroidogenic gene expression (Windak et al., 2013; Lan et al., 2007), were enriched in both hiPSC-CMs and NRVMs. Both cell types also had an enriched binding site for transcription factor E2-alpha (TCF3) and for nuclear factor erythroid-derived 2 (NFE2). In hiPSC-CMs, two binding sites for myocyte enhancer Factor 2A (MEF2A) were enriched. MEF2A is known to regulate multiple cardiac structural genes and to be activated by several hypertrophic signaling pathways (Czubryt and Olson, 2004; Xu et al., 2006; Han and Molkentin, 2000). In NRVMs, two binding sites for both MYC proto-oncogene protein and heat shock transcription factor 1 (HSF1) were enriched.

Differentially expressed lncRNAs

Of the 7,818 long noncoding RNAs (lncRNAs) expressed in our samples, only one lncRNA was differentially expressed after 24 h of stretch: *LINC00648* was downregulated by 50% (p=0.011) relative to the unstretched control. *LINC00648* also showed downregulation by 30% in hESC-CMs after a 48-h stretch (Ovchinnikova et al., 2018). In hiPSC-CMs, after 48 h of stretch, one lncRNA (*LINC00702*) was upregulated, while five lncRNAs (*AUXG01000058.1, AZIN1-AS1, LAMTOR5-AS1, LINC01341, PTPRG-AS1*) were downregulated. There is no previous report of these lncRNAs being involved in cardiomyocyte hypertrophy. Predicted putative interaction partners of the differentially expressed lncRNAs are shown in Table S4. None of these interaction partners was differentially expressed (>1.5-fold) in response to stretch. However, an interaction partner of *AZIN1-AS1*, a gene encoding Egl-9 family hypoxia inducible factor 3 (*EGLN3),* was upregulated 1.48-fold (p=0.0454).

EGLN3 is a prolyl hydroxylase that is activated by hypoxia and may regulate cardiomyocyte apoptosis (Liu et al., 2010).

The effects of p38 MAPK, MEK1/2, PKC and BET inhibition on the stretch response

To gain further insight into the signaling routes mediating the stretch response in hiPSC-CMs, the involvement of p38 MAPK, MEK1/2 and PKC signaling pathways as well as BET in the stretch response of hiPSC-CMs was examined by pharmacological inhibitors and analysis of *NPPA* and *NPPB* mRNA expression after mechanical stretch for 24 h. In this experiment, *NPPA* expression was not significantly affected by stretch, while a 5.6-fold increase (p=0.008) in *NPPB* expression was detected in 0.1% DMSO-treated stretched cells compared to unstretched cells (Fig. 7). The MEK1/2 inhibitor U0126 at a concentration of 10 µM decreased both *NPPA* and *NPPB* gene expression (40%, p=0.008 and 80%, p=0.008, respectively), while the cPKC inhibitor Gö6976 at 1 µM increased *NPPB* expression 1.8-fold (p=0.016). In addition, the p38 MAPK inhibitor SB203580 at 10 µM and the BET inhibitor JQ1 at 300 nM showed a tendency toward increased *NPPA* and *NPPB* expression. An inhibitor of all PKC isoforms, Gö6983 at 1 µM, did not affect basal *NPPA* or *NPPB* gene expression.

The effect of compounds on the stretch-induced hypertrophic response was evaluated by *NPPB* expression (Fig. 7B). None of the treatments could fully block the stretch response, although U0126 significantly decreased stretch-induced *NPPB* expression compared to DMSO-treated stretched cells (70%, p=0.016). SB203580 and Gö6976 slightly increased the *NPPB* stretch response relative to DMSO, while Gö6983 tended to decrease it. The BET inhibitor JQ1 did not affect the stretch-induced increase in *NPPB* expression.

Discussion

Prolonged mechanical load leads to maladaptive changes in the heart, including cardiomyocyte hypertrophy and left ventricular hypertrophy, which are major causes of heart failure (Heineke and Molkentin, 2006). Understanding the molecular mechanisms that underlie the development of left ventricular hypertrophy is essential for finding new treatments for heart failure. Identification of genes and pathways involved mechanical stretch response of cardiomyocytes is therefore of great interest.

The optimal *in vitro* model of cardiomyocyte hypertrophy would use adult human cardiomyocytes. However, they are difficult to obtain and culture long-term, so the most commonly used *in vitro* hypertrophy models employ NRVMs. To study this phenomenon in human cells and reduce the use of experimental animals, we used hiPSC-CMs. *In vitro* models of hiPSC-CMs are increasingly used in disease modeling and drug development (Ovics et al., 2020; Protze et al., 2019; Karakikes et al., 2015). To our knowledge, the transcriptional responses of hiPSC-CMs to cyclic mechanical stretch have not been characterized before. We validated the model by measuring the expression of well-

established mechanical stress-responsive genes, *NPPA* and *NPPB* (Ogawa et al., 1995), and showed that cyclic mechanical stretch leads to *NPPA* and *NPPB* gene expression responses comparable to those of NRVMs (Pikkarainen et al., 2003; Rysä et al., 2018).

We then performed RNAseq to identify additional gene expression changes involved in the hypertrophic response. Surprisingly, the number of differentially expressed genes in the stretched hiPSC-CMs was drastically lower than in the stretched NRVMs or hESC-CMs (Ovchinnikova et al., 2018; Rysä et al., 2018). In the NRVM study (Rysä et al., 2018), the species difference and the different methods (microarray in the NRVM study and RNAseq in the present hiPSC-CM analysis) may partly explain the difference. Furthermore, the hiPSC-CM cultures used in the current analysis were ≥95% pure cardiomyocytes, while NRVMs isolated from the heart usually contain other cardiac cell types, such as fibroblasts and endothelial cells, despite enrichment with preplating. In agreement with this, a broad range of gene expression changes was observed in NRVMs, including several changes associated with cardiac fibroblast activation such as upregulation of α-smooth muscle actin (*ACTA2*), a hallmark of fibroblast activation, and overrepresentation of GO terms of extracellular matrix and collagen-containing extracellular matrix. Similar changes in gene expression were not detected in stretched hiPSC-CM, suggesting that pure cardiomyocyte cultures are more suitable to study the changes occurring specifically in cardiomyocytes. In the hESC-CM study (Ovchinnikova et al., 2018), >98% pure cardiomyocytes were used, but the magnitude and frequency of the stretch applied were different. Moreover, the age and maturation level of the cardiomyocytes were not described in the hESC-CM study, and these differences may influence the comparison of the two human cardiomyocyte models. Although transcriptionally hESC-CMs and hiPSC-CMs are very similar (Gupta et al., 2010), their responses to stretch were different. As NRVMs, hESC-CMs also seem to respond to stretching by inducing a broad range of gene expression changes, while in hiPSC-CMs, differentially expressed genes are more defined. Only one gene, *TUBB2B*, coding for tubulin beta-2A chain, a constituent of microtubules, was upregulated in all cardiomyocyte types. In hiPSC-CMs, other forms of alpha- and beta-tubulins were also upregulated. The increase in the expression of microtubules is strongly associated with cardiac hypertrophy; thus, this change was expected (Caporizzo et al., 2019). In contrast, one gene, *ZNF519*, coding for zinc finger protein 519, was downregulated in all cell models. *ZNF519* has not been characterized in cardiomyocytes, and its potential role in the development of cardiomyocyte hypertrophy remains to be established.

In response to stretch, two central changes occur in cardiomyocytes: (1) several genes normally expressed only in embryonic or fetal hearts are reactivated, and (2) the expression of sarcomeric and other constitutive proteins is increased (Kuwahara et al., 2012; Hoshijima and Chien, 2002). Here, we showed that these changes occur also in hiPSC-CMs in response to stretching. The upregulation of

contractile proteins was also reflected in the GO enrichment analysis, where most enriched processes were associated with actin-myosin filament sliding and muscle contraction.

Although the differentially expressed genes and their numbers differed among the studies using different cardiomyocyte models, some similarities in the enriched processes and pathways were discovered. Regulation of cell death and sterol biosynthesis were enriched in the upregulated genes in all cell types. Apoptosis has previously been linked to hypertrophy in multiple studies both in rodents and in humans (Okada et al., 2004; Mohamed et al., 2016; Fujita and Ishikawa, 2011; Condorelli et al., 1999). Although the upregulation of genes associated with steroid biosynthesis has been reported in previous studies (Rysä et al., 2018; Ovchinnikova et al., 2018), its role in cardiomyocyte hypertrophy has not been characterized. Increased steroid synthesis might be needed for the growth of cardiomyocytes or may be associated with changes in energy metabolism. Steroid biosynthesis is downregulated in the neonatal mouse heart within the first nine days of postnatal life, during which the heart loses its regenerative capacity (Talman et al., 2018). Hence, it can be speculated that increased steroid synthesis is a part of the fetal program that is reactivated in response to stress.

Several genes associated with both apoptosis and cardiomyocyte hypertrophy, such as *CRYAB*, *ENO1* and *GSTO1*, were among the upregulated genes in hiPSC-CMs (Kumarapeli et al., 2008; Chis et al., 2012; Captur et al., 2020; Dulhunty et al., 2001; Piaggi et al., 2010; Manupati et al., 2019; Wang, K. et al., 2021; Wang, L. et al., 2019). *ENO1*, which codes for the glycolytic enzyme α-enolase and is normally highly expressed in embryonic and fetal heart but only weakly in adult heart, has shown to increase during hypertrophy in animal models (Gao et al., 2018; Keller et al., 1995; Zhu et al., 2009). This is in line with previous evidence of a metabolic switch from fatty acid to glycolysis during pathological hypertrophy (Lehman and Kelly, 2002). Furthermore, one study has shown compensatory increase in α-enolase expression to protect cardiomyocytes from hypertrophy (Gao et al., 2018). Interestingly, after a 48-h stretch, the most upregulated genes were neuropeptide galanin and GMAP prepropeptide coding gene *GAL*. Galanin is expressed mainly in the nervous system and in some peripheral organs, but no expression in cardiomyocytes has been reported (Palkeeva et al., 2019). However, its receptors are expressed in various cell types, including cardiomyocytes, and it has been suggested to be cardioprotective (Fang et al., 2013; Studneva et al., 2020; Serebryakova et al., 2019; Palkeeva et al., 2019; Martinelli et al., 2021).

All cardiomyocyte types included in the present comparisons, hiPSC-CMs, hESC-CMs and NRVMs, are considered relatively immature and do not fully correspond to adult cardiomyocytes in terms of their sarcomere structure, metabolism, or electrophysiological properties (Robertson et al., 2013). However, based on our comparison, stretched hiPSC-CMs were the only cell model in which biological processes of muscle contraction and actin-myosin filament sliding were enriched among the upregulated genes. In view of *in vivo* cardiac overload, these are the most important processes to

enhance in order to preserve cardiac pump function. However, these changes could also imply maturation of hiPSC-CMs, but this is unlikely because they were accompanied by upregulation of the fetal gene program and apoptosis-associated genes. Moreover, hiPSC-CMs were the only cells in which upregulated genes had enrichment of pathways for hypertrophic cardiomyopathy. On the contrary, these pathways were enriched among downregulated genes of stretched hESC-CMs (Ovchinnikova et al., 2018). Taken together, hiPSC-CMs show distinct hypertrophic changes in gene expression at the levels of individual genes and biological processes, indicating that cyclic stretching of hiPSC-CMs is an advantageous *in vitro* model for studying mechanically induced cardiomyocyte hypertrophy.

Finally, we applied our model to study signaling pathways associated with cardiomyocyte hypertrophy. Although p38 MAPK, MEK1/2-ERK1/2, PKC and BET are widely studied in animal models, their role in human cardiomyocytes is poorly known. In this study, the tested inhibitors of these transducers could not block the *NPPB* stretch response completely, indicating that these signaling pathways are not necessary for mechanical stretch-induced hypertrophy of hiPSC-CMs. Previous studies using MEK1/2 and BET inhibitors have demonstrated that MEK1/2 and BET mediate ET-1-induced proBNP and *NPPB* expression in hiPSC-CMs (Pohjolainen et al., 2020; Duan et al., 2017). Thus, in hiPSC-CMs, ET-1 and mechanical stimulation seem to induce BNP expression through different signaling pathways.

In conclusion, in the present study, we showed that mechanical stretching of hiPSC-CMs is a relevant *in vitro* model for studying human cardiomyocyte hypertrophy. We elucidated stretch-induced transcriptional changes and identified biological processes and pathways associated with these gene expression changes. The changes, including activation of the fetal gene program and upregulation of constitutive protein coding genes, were characteristic of cardiomyocyte hypertrophy. Comparison to previous data of stretched NRVMs and hESC-CMs demonstrated that hiPSC-CMs revealed more defined changes in gene expression and that differentially expressed genes were restricted to cardiac and hypertrophy-related genes. In addition, we identified several differentially expressed genes with no or weak previous association with cardiomyocyte hypertrophy. These results can be used to further elucidate hypertrophic signaling pathways and to discover potential pharmacological targets and biomarkers of cardiomyocyte hypertrophy.

Materials and Methods

Compounds and reagents

The MEK1/2 inhibitor U0126 and the p38 MAPK inhibitor SB203580 were purchased from Tocris Bioscience (Bristol, UK), the pan-PKC inhibitor Gö6983 was purchased from STEMCELL

Technologies (Vancouver, Canada), and the classical PKC inhibitor Gö6976 and the BET inhibitor JQ1 were purchased from Merck (Darmstadt, Germany). Growth factor-reduced Matrigel was purchased from Corning (Bedford, MA, USA), and the small-molecule inhibitors Y-27632, CHIR99021 and Wnt-C59 were purchased from Tocris Bioscience (Bristol, UK). All other cell culture reagents were purchased from Gibco (Paisley, UK).

Human induced pluripotent stem cell-derived cardiomyocytes

The hiPS(IMR90)-4 line was purchased from WiCell (Madison, WI, USA). Cells were maintained in Essential 8 medium on Matrigel-coated 6-well plates at 37 °C in a humidified atmosphere of 5% CO_2. Cells were passaged 1:15 approximately every four days using Versene and regularly tested negative for mycoplasma contamination. Cardiomyocytes were differentiated as described previously (Pohjolainen et al., 2020; Burridge et al., 2014; Karhu et al., 2018). When the cultures were 80-95% confluent, differentiation was initiated by the addition of 6 µM CHIR99021 (Day 0) to RPMI 1640 medium supplemented with B-27 without insulin (RB-). On Day 1 or Day 2, the medium was changed to fresh RB-. On Day 3, fresh RB- containing 2.5 µM Wnt-C59 was added. On Days 5, 7 and 9, RB- was changed to fresh RB-. On Day 11, metabolic selection of cardiomyocytes was started by changing the RB- to RPMI 1640 without glucose supplemented with B-27 (with insulin). On Day 13, the cells were fed fresh metabolic selection medium. From Day 15 onwards, the cardiomyocytes were cultured in RPMI 1640 supplemented with B-27 (RB+). On Days 15 or 17, the differentiated hiPSC-CMs were dissociated and seeded at a density of 700,000-800,000 cells/well in RB+ supplemented with 10% fetal bovine serum on flexible collagen I-coated 6-well BioFlex® culture plates (Flexcell International Corporation, Hillsborough, NC, USA) with additional Matrigel coating. The hiPSC-CMs were allowed to attach for 48 h, after which the medium was changed to serum-free RB+. Cardiomyocytes were maintained by changing fresh RB+ approximately every four days until the start of experiments on Days 29-43.

Cyclic mechanical stretch

The hiPSC-CMs were exposed to cyclic mechanical stretch by applying vacuum suction to the BioFlex® plates with an FX-5000 Tension System (Flexcell International Corporation). For pharmacological assays, compounds were added one hour before starting the stretch. Equibiaxial stretch was applied for 24 h, 48 h or 72 h in two-second cycles (0.5 Hz) to induce 10 to 21% stretch. Unstretched control cells were from the same differentiation and were seeded on BioFlex® plates at the same time, but no stretch was applied.

RNA isolation

Cells were lysed in 350 µl of RA1 lysis buffer (Macherey-Nagel, Düren, Germany) supplemented with 1% β-mercaptoethanol and stored at -80 °C (maximum one month) before RNA isolation. RNA was isolated using a NucleoSpin RNA kit (Macherey-Nagel) according to the manufacturer's instructions. Analysis of the RNA concentration and quality was performed with a NanoDrop 1000 spectrophotometer (Thermo Fisher Scientific, Waltham, MA, USA) for qRT-PCR and with 4200 TapeStation (Agilent, Santa Clara, CA, USA) for RNAseq. One of the sample pairs at 24 h time point was omitted from the RNAseq due to poor quality (RNA integrity number < 9).

Quantitative Reverse Transcription PCR (qRT-PCR)

cDNA was synthesized from 100–500 ng of total RNA in 10 µl reactions with a Transcriptor First Strand cDNA Synthesis Kit (Roche, Basel, Switzerland) according to the manufacturer's protocol using random hexamer primers and an MJ Mini Personal thermal cycler (Bio-Rad, Hercules, CA, USA). The cDNA was diluted 1:10 in PCR grade H_2O and stored at -20 °C. Commercial TaqMan® Gene Expression Assays (Thermo Fisher Scientific) listed in Table S1 were used with LightCycler® 480 Probes Master reagent (Roche) according to the manufacturer's instructions. A LightCycler® 480 Real-Time PCR System (Roche) was used to analyze 4.5 µl of the cDNA dilution in 10 µl reactions on a white LightCycler® 480 Multiwell Plate 384 (Roche). To confirm the absence of PCR contamination, no-template controls were used. Each reaction was run at least in triplicate, and the average of the technical replicates was used in the analysis as n=1. Grubbs' test was used to identify outliers within technical replicates and identified outliers were excluded from the analysis. The $2^{-\Delta\Delta Ct}$ method was used to analyze the relative gene expression using *ACTB* and *18S rRNA* as reference genes.

RNA sequencing

RNAseq was performed as single-end sequencing for a read length of 75 bp with an Illumina NextSeq 500 sequencer (Illumina, San Diego, CA, USA) in high output runs using a NEBNext Ultra Directional RNA Library Prep kit (New England Biolabs, Ipswich, MA, USA) including rRNA depletion. Data quality was analyzed by FastQC, and quality trimming was applied to the data with Trimmomatic software (Bolger et al., 2014). The sample reads were aligned against the Genome Reference Consortium Human Build 38 patch release 13 (GRCh38.p13, GCA_000001405.28) reference with Spliced Transcripts Alignment to a Reference (STAR) (Dobin et al., 2013). The mapping quality was assessed with Qualimap (Okonechnikov et al., 2016). Read quantification was created with featureCounts (Liao, Yang et al., 2014), and differential expression with quality assessment was performed with DESeq2 (Love et al., 2014).

Functional enrichment analysis of gene sets

GO enrichment of differentially expressed genes was analyzed with GOrilla (version updated 27th of February 2021, available at http://cbl-gorilla.cs.technion.ac.il/) (Eden et al., 2009). The tool searched for GO terms that were enriched in the target set compared to the background set. A list of upregulated or downregulated genes was entered as target sets. As the background set, we used all expressed genes in our dataset (30,861 genes), defined as genes with a detected signal in at least two samples in one treatment group. A relatively low p value threshold of $p<0.0001$ was used for running the analysis, as no correction for multiple testing was applied. FDR-adjusted p values were calculated after the analysis, and an FDR-adjusted p value <0.05 was considered significant.

WebGestalt (version 2019, available at http://www.webgestalt.org/) was used for KEGG and Reactome pathway analyses and for transcription factor target analysis (Liao, Yuxing et al., 2019). The same target and reference gene sets as in the GO enrichment analysis were used. The Benjamini-Hochberg method was used for multiple testing, and a significance level of <0.05 was used. KEGG Mapper (available at https://www.genome.jp/kegg/mapper.html) was used to determine the cellular functions of proteins representing the differentially expressed genes [24]. Encyclopedia of RNA Interactomes (ENCORI; available at http://starbase.sysu.edu.cn/) was used to predict the putative interaction partners of differentially expressed lncRNAs (Li et al., 2014).

Dataset comparison

Our dataset of stretched hiPSC-CMs was compared to datasets of the two other studies. We used data from differentially expressed genes of stretched NRVMs by Rysä et al. (Rysä et al., 2018), who isolated NRVMs from 2- to 4-day-old Sprague–Dawley rats and stretched cells with the FlexCell vacuum system, similar to the present study (0.5 Hz, 10-25% elongation). We also compared our data to the data of stretched hESC-CMs obtained by Ovchinnikova et al. (Ovchinnikova et al., 2018), who had used a slightly different stretching protocol: cyclic stretch with elongation from 0% to 15% was applied at a frequency of 1 Hz with the FlexCell system.

Statistical analysis

Each treatment group comprised 3–5 independent experiments of cells from individual differentiations. Sample size was determined by initial analysis of *NPPA* and *NPPB* responses measured by qRT-PCR and previous study on NRVMs (Rysä et al., 2018). Each qRT-PCR included technical replicates, and the average was calculated for statistical analysis to represent n=1. Statistical analysis of the qRT-PCR results was performed in IBM SPSS Statistics 25 software. Student's t-test for independent samples was performed to compare the stretched and unstretched samples. A nonparametric Mann–Whitney U test was applied for the normalized qRT-PCR data of the

pharmacological inhibitor experiments. A value of $p<0.05$ was considered statistically significant. Statistical analysis of the RNAseq results was performed as a pairwise comparison of stretched and unstretched samples using the Wald test in DESeq2 software. Genes with a fold change (FC) >1.5 and Benjamini-Hochberg adjusted $p<0.05$ were defined as differentially expressed.

Acknowledgements

We thank Ms Annika Korvenpää and Ms Ángela Morujo for their technical assistance. The RNAseq was provided by the Biomedicum Functional Genomics Unit at the Helsinki Institute of Life Science and Biocenter Finland at the University of Helsinki. We thank American Journal Experts (AJE) for English language editing.

Competing interests

No competing interests declared.

Funding

This work was supported by the Academy of Finland [grants 321564, 328909], the Finnish Foundation for Cardiovascular Research, Sigrid Jusélius Foundation, University of Helsinki Research Funds, and Doctoral Programme in Drug Research.

Data Availability Statement

The RNAseq data are freely available at the NCBI Gene Expression Omnibus (http://www.ncbi.nlm.nih.gov/geo, accession number GSE186208). All other data are available from the corresponding author upon reasonable request.

Author contributions statement

Lotta Pohjolainen: Conceptualization, Methodology, Validation, Formal analysis, Investigation, Writing – original draft preparation

Heikki Ruskoaho: Conceptualization, Methodology, Writing – review and editing, Supervision, Project administration, Funding acquisition

Virpi Talman: Conceptualization, Methodology, Writing – review and editing, Supervision, Project administration, Funding acquisition

References

Bolger, A.M., Lohse, M. and Usadel, B. (2014). Trimmomatic: a flexible trimmer for Illumina sequence data. *Bioinformatics* **30**, 2114-2120.

Borck, P.C., Guo, L. and Plutzky, J. (2020). BET Epigenetic Reader Proteins in Cardiovascular Transcriptional Programs. *Circ Res* **126**, 1190-1208.

Burridge, P.W., Matsa, E., Shukla, P., Lin, Z.C., Churko, J.M., Ebert, A.D., Lan, F., Diecke, S., Huber, B., Mordwinkin, N.M., et al. (2014). Chemically defined generation of human cardiomyocytes. *Nat. Methods* **11**, 855-860.

Caporizzo, M.A., Chen, C.Y. and Prosser, B.L. (2019). Cardiac microtubules in health and heart disease. *Exp Biol Med (Maywood)* **244**, 1255-1272.

Captur, G., Heywood, W.E., Coats, C., Rosmini, S., Patel, V., Lopes, L.R., Collis, R., Patel, N., Syrris, P., Bassett, P., et al. (2020). Identification of a Multiplex Biomarker Panel for Hypertrophic Cardiomyopathy Using Quantitative Proteomics and Machine Learning. *Mol Cell Proteomics* **19**, 114-127.

Carlson, C., Koonce, C., Aoyama, N., Einhorn, S., Fiene, S., Thompson, A., Swanson, B., Anson, B. and Kattman, S. (2013). Phenotypic screening with human iPS cell-derived cardiomyocytes: HTS-compatible assays for interrogating cardiac hypertrophy. *J Biomol Screen* **18**, 1203-1211.

Chis, R., Sharma, P., Bousette, N., Miyake, T., Wilson, A., Backx, P.H. and Gramolini, A.O. (2012). α-Crystallin B prevents apoptosis after H2O2 exposure in mouse neonatal cardiomyocytes. *Am J Physiol Heart Circ Physiol* **303**, 967.

Coletti, D., Daou, N., Hassani, M., Li, Z. and Parlakian, A. (2016). Serum Response Factor in Muscle Tissues: From Development to Ageing. *Eur J Transl Myol* **26**, 6008.

Condorelli, G., Morisco, C., Stassi, G., Notte, A., Farina, F., Sgaramella, G., de Rienzo, A., Roncarati, R., Trimarco, B. and Lembo, G. (1999). Increased cardiomyocyte apoptosis and changes in proapoptotic and antiapoptotic genes bax and bcl-2 during left ventricular adaptations to chronic pressure overload in the rat. *Circulation* **99**, 3071-3078.

Czubryt, M.P. and Olson, E.N. (2004). Balancing contractility and energy production: the role of myocyte enhancer factor 2 (MEF2) in cardiac hypertrophy. *Recent Prog Horm Res* **59**, 105-124.

Dobin, A., Davis, C.A., Schlesinger, F., Drenkow, J., Zaleski, C., Jha, S., Batut, P., Chaisson, M. and Gingeras, T.R. (2013). STAR: ultrafast universal RNA-seq aligner. *Bioinformatics* **29**, 15-21.

Duan, Q., McMahon, S., Anand, P., Shah, H., Thomas, S., Salunga, H.T., Huang, Y., Zhang, R., Sahadevan, A., Lemieux, M.E., et al. (2017). BET bromodomain inhibition suppresses innate inflammatory and profibrotic transcriptional networks in heart failure. *Sci Transl Med* **9**.

Dulhunty, A., Gage, P., Curtis, S., Chelvanayagam, G. and Board, P. (2001). The glutathione transferase structural family includes a nuclear chloride channel and a ryanodine receptor calcium release channel modulator. *J Biol Chem* **276**, 3319-3323.

Eden, E., Navon, R., Steinfeld, I., Lipson, D. and Yakhini, Z. (2009). GOrilla: a tool for discovery and visualization of enriched GO terms in ranked gene lists. *BMC Bioinformatics* **10**, 48.

Fang, P., Sun, J., Wang, X., Zhang, Z., Bo, P. and Shi, M. (2013). Galanin participates in the functional regulation of the diabetic heart. *Life Sci* **92**, 628-632.

Földes, G., Matsa, E., Kriston-Vizi, J., Leja, T., Amisten, S., Kolker, L., Kodagoda, T., Dolatshad, N.F., Mioulane, M., Vauchez, K., et al. (2014). Aberrant α-adrenergic hypertrophic response in cardiomyocytes from human induced pluripotent cells. *Stem Cell Reports* **3**, 905-914.

Frey, N., Katus, H.A., Olson, E.N. and Hill, J.A. (2004). Hypertrophy of the heart: a new therapeutic target? *Circulation* **109**, 1580-1589.

Fujita, T. and Ishikawa, Y. (2011). Apoptosis in heart failure. -The role of the β-adrenergic receptor-mediated signaling pathway and p53-mediated signaling pathway in the apoptosis of cardiomyocytes-. *Circ J* **75**, 1811-1818.

Gao, S., Liu, X., Wei, L., Lu, J. and Liu, P. (2018). Upregulation of α-enolase protects cardiomyocytes from phenylephrine-induced hypertrophy. *Can J Physiol Pharmacol* **96**, 352-358.

Gupta, M.K., Illich, D.J., Gaarz, A., Matzkies, M., Nguemo, F., Pfannkuche, K., Liang, H., Classen, S., Reppel, M., Schultze, J.L., et al. (2010). Global transcriptional profiles of beating clusters derived from human induced pluripotent stem cells and embryonic stem cells are highly similar. *BMC Dev Biol* **10**, 98.

Han, J. and Molkentin, J.D. (2000). Regulation of MEF2 by p38 MAPK and its implication in cardiomyocyte biology. *Trends Cardiovasc Med* **10**, 19-22.

Heineke, J. and Molkentin, J.D. (2006). Regulation of cardiac hypertrophy by intracellular signalling pathways. *Nat. Rev. Mol. Cell Biol.* **7**, 589-600.

Hoshijima, M. and Chien, K.R. (2002). Mixed signals in heart failure: cancer rules. *J Clin Invest* **109**, 849-855.

Karakikes, I., Ameen, M., Termglinchan, V. and Wu, J.C. (2015). Human induced pluripotent stem cell-derived cardiomyocytes: insights into molecular, cellular, and functional phenotypes. *Circulation Research* **117**, 80-88.

Karhu, S.T., Välimäki, M.J., Jumppanen, M., Kinnunen, S.M., Pohjolainen, L., Leigh, R.S., Auno, S., Földes, G., Boije Af Gennäs, G., Yli-Kauhaluoma, J., et al. (2018). Stem cells are the most sensitive screening tool to identify toxicity of GATA4-targeted novel small-molecule compounds. *Arch. Toxicol.* **92**, 2897-2911.

Keller, A., Rouzeau, J.D., Farhadian, F., Wisnewsky, C., Marotte, F., Lamandé, N., Samuel, J.L., Schwartz, K., Lazar, M. and Lucas, M. (1995). Differential expression of alpha- and beta-enolase genes during rat heart development and hypertrophy. *Am J Physiol* **269**, 1843.

Kohli, S., Ahuja, S. and Rani, V. (2011). Transcription factors in heart: promising therapeutic targets in cardiac hypertrophy. *Curr Cardiol Rev* **7**, 262-271.

Kumarapeli, A.R.K., Su, H., Huang, W., Tang, M., Zheng, H., Horak, K.M., Li, M. and Wang, X. (2008). Alpha B-crystallin suppresses pressure overload cardiac hypertrophy. *Circ Res* **103**, 1473-1482.

Kuwahara, K., Nishikimi, T. and Nakao, K. (2012). Transcriptional regulation of the fetal cardiac gene program. *J Pharmacol Sci* **119**, 198-203.

Lan, H., Li, H., Lin, G., Lai, P. and Chung, B. (2007). Cyclic AMP stimulates SF-1-dependent CYP11A1 expression through homeodomain-interacting protein kinase 3-mediated Jun N-terminal kinase and c-Jun phosphorylation. *Mol Cell Biol* **27**, 2027-2036.

Lehman, J.J. and Kelly, D.P. (2002). Gene regulatory mechanisms governing energy metabolism during cardiac hypertrophic growth. *Heart Fail Rev* **7**, 175-185.

Li, J., Liu, S., Zhou, H., Qu, L. and Yang, J. (2014). starBase v2.0: decoding miRNA-ceRNA, miRNA-ncRNA and protein-RNA interaction networks from large-scale CLIP-Seq data. *Nucleic Acids Res* **42**, 92.

Liao, Y., Smyth, G.K. and Shi, W. (2014). featureCounts: an efficient general purpose program for assigning sequence reads to genomic features. *Bioinformatics* **30**, 923-930.

Liao, Y., Wang, J., Jaehnig, E.J., Shi, Z. and Zhang, B. (2019). WebGestalt 2019: gene set analysis toolkit with revamped UIs and APIs. *Nucleic Acids Res* **47**, W199-W205.

Liu, Y., Huo, Z., Yan, B., Lin, X., Zhou, Z., Liang, X., Zhu, W., Liang, D., Li, L., Liu, Y., et al. (2010). Prolyl hydroxylase 3 interacts with Bcl-2 to regulate doxorubicin-induced apoptosis in H9c2 cells. *Biochem Biophys Res Commun* **401**, 231-237.

Lorell, B.H. and Carabello, B.A. (2000). Left ventricular hypertrophy: pathogenesis, detection, and prognosis. *Circulation* **102**, 470-479.

Love, M.I., Huber, W. and Anders, S. (2014). Moderated estimation of fold change and dispersion for RNA-seq data with DESeq2. *Genome Biol* **15**, 550.

Manupati, K., Debnath, S., Goswami, K., Bhoj, P.S., Chandak, H.S., Bahekar, S.P. and Das, A. (2019). Glutathione S-transferase omega 1 inhibition activates JNK-mediated apoptotic response in breast cancer stem cells. *FEBS J* **286**, 2167-2192.

Martinelli, I., Timotin, A., Moreno-Corchado, P., Marsal, D., Kramar, S., Loy, H., Joffre, C., Boal, F., Tronchere, H. and Kunduzova, O. (2021). Galanin promotes autophagy and alleviates apoptosis in the hypertrophied heart through FoxO1 pathway. *Redox Biol* **40**, 101866.

Mohamed, B.A., Schnelle, M., Khadjeh, S., Lbik, D., Herwig, M., Linke, W.A., Hasenfuss, G. and Toischer, K. (2016). Molecular and structural transition mechanisms in long-term volume overload. *Eur J Heart Fail* **18**, 362-371.

Nelson, T.J., Balza, R., Xiao, Q. and Misra, R.P. (2005). SRF-dependent gene expression in isolated cardiomyocytes: regulation of genes involved in cardiac hypertrophy. *J Mol Cell Cardiol* **39**, 479-489.

Ogawa, Y., Itoh, H. and Nakao, K. (1995). Molecular biology and biochemistry of natriuretic peptide family. *Clin Exp Pharmacol Physiol* **22**, 49-53.

Okada, K., Minamino, T., Tsukamoto, Y., Liao, Y., Tsukamoto, O., Takashima, S., Hirata, A., Fujita, M., Nagamachi, Y., Nakatani, T., et al. (2004). Prolonged endoplasmic reticulum stress in hypertrophic and failing heart after aortic constriction: possible contribution of endoplasmic reticulum stress to cardiac myocyte apoptosis. *Circulation* **110**, 705-712.

584 **Okonechnikov, K., Conesa, A. and García-Alcalde, F.** (2016). Qualimap 2: advanced multi-sample
585 quality control for high-throughput sequencing data. *Bioinformatics* **32**, 292-294.

586 **Ovchinnikova, E., Hoes, M., Ustyantsev, K., Bomer, N., de Jong, T.V., van der Mei, H.,**
587 **Berezikov, E. and van der Meer, P.** (2018). Modeling Human Cardiac Hypertrophy in Stem
588 Cell-Derived Cardiomyocytes. *Stem Cell Reports* **10**, 794-807.

589 **Ovics, P., Regev, D., Baskin, P., Davidor, M., Shemer, Y., Neeman, S., Ben-Haim, Y. and Binah,**
590 **O.** (2020). Drug Development and the Use of Induced Pluripotent Stem Cell-Derived
591 Cardiomyocytes for Disease Modeling and Drug Toxicity Screening. *Int J Mol Sci* **21**, E7320.

592 **Palaniyandi, S.S., Sun, L., Ferreira, J.C.B. and Mochly-Rosen, D.** (2009). Protein kinase C in heart
593 failure: a therapeutic target? *Cardiovasc Res* **82**, 229-239.

594 **Palkeeva, M., Studneva, I., Molokoedov, A., Serebryakova, L., Veselova, O., Ovchinnikov, M.,**
595 **Sidorova, M. and Pisarenko, O.** (2019). Galanin/GalR1-3 system: A promising therapeutic
596 target for myocardial ischemia/reperfusion injury. *Biomed Pharmacother* **109**, 1556-1562.

597 **Piaggi, S., Raggi, C., Corti, A., Pitzalis, E., Mascherpa, M.C., Saviozzi, M., Pompella, A. and**
598 **Casini, A.F.** (2010). Glutathione transferase omega 1-1 (GSTO1-1) plays an anti-apoptotic role
599 in cell resistance to cisplatin toxicity. *Carcinogenesis* **31**, 804-811.

600 **Pikkarainen, S., Tokola, H., Majalahti-Palviainen, T., Kerkela, R., Hautala, N., Bhalla, S.S.,**
601 **Charron, F., Nemer, M., Vuolteenaho, O. and Ruskoaho, H.** (2003). GATA-4 is a nuclear
602 mediator of mechanical stretch-activated hypertrophic program. *J Biol Chem* **278**, 23807-23816.

603 **Pohjolainen, L., Easton, J., Solanki, R., Ruskoaho, H. and Talman, V.** (2020). Pharmacological
604 Protein Kinase C Modulators Reveal a Pro-hypertrophic Role for Novel Protein Kinase C
605 Isoforms in Human Induced Pluripotent Stem Cell-Derived Cardiomyocytes. *Front Pharmacol*
606 **11**, 553852.

607 **Protze, S.I., Lee, J.H. and Keller, G.M.** (2019). Human Pluripotent Stem Cell-Derived
608 Cardiovascular Cells: From Developmental Biology to Therapeutic Applications. *Cell Stem Cell*
609 **25**, 311-327.

610 **Robertson, C., Tran, D.D. and George, S.C.** (2013). Concise review: maturation phases of human
611 pluripotent stem cell-derived cardiomyocytes. *Stem Cells* **31**, 829-837.

612 **Rose, B.A., Force, T. and Wang, Y.** (2010). Mitogen-activated protein kinase signaling in the heart:
613 angels versus demons in a heart-breaking tale. *Physiol Rev* **90**, 1507-1546.

Roth, G.A., Johnson, C., Abajobir, A., Abd-Allah, F., Abera, S.F., Abyu, G., Ahmed, M., Aksut, B., Alam, T., Alam, K., et al. (2017). Global, Regional, and National Burden of Cardiovascular Diseases for 10 Causes, 1990 to 2015. *Journal of the American College of Cardiology* **70**, 1-25.

Rysä, J., Tokola, H. and Ruskoaho, H. (2018). Mechanical stretch induced transcriptomic profiles in cardiac myocytes. *Sci Rep* **8**, 4733.

Serebryakova, L., Pal'keeva, M., Studneva, I., Molokoedov, A., Veselova, O., Ovchinnikov, M., Gataulin, R., Sidorova, M. and Pisarenko, O. (2019). Galanin and its N-terminal fragments reduce acute myocardial infarction in rats. *Peptides* **111**, 127-131.

Studneva, I.M., Veselova, O.M., Bahtin, A.A., Konovalova, G.G., Lankin, V.Z. and Pisarenko, O.I. (2020). The Mechanisms of Cardiac Protection Using a Synthetic Agonist of Galanin Receptors during Chronic Administration of Doxorubicin. *Acta Naturae* **12**, 89-98.

Talman, V., Teppo, J., Pöhö, P., Movahedi, P., Vaikkinen, A., Karhu, S.T., Trošt, K., Suvitaival, T., Heikkonen, J., Pahikkala, T., et al. (2018). Molecular Atlas of Postnatal Mouse Heart Development. *J Am Heart Assoc* **7**, e010378.

University of Washington, Institute of Health Metrics and Evaluation (2021). GBD Results Tool. http://ghdx.healthdata.org/gbd-results-tool.

Wang, K., Zhang, F. and Jia, W. (2021). Glutathione S-transferase ω 1 promotes the proliferation, migration and invasion, and inhibits the apoptosis of non-small cell lung cancer cells, via the JAK/STAT3 signaling pathway. *Mol Med Rep* **23**.

Wang, L., Yue, H., Peng, X. and Zhang, S. (2019). GSTO1 regards as a meritorious regulator in cutaneous malignant melanoma cells. *Mol Cell Probes* **48**, 101449.

Windak, R., Müller, J., Felley, A., Akhmedov, A., Wagner, E.F., Pedrazzini, T., Sumara, G. and Ricci, R. (2013). The AP-1 transcription factor c-Jun prevents stress-imposed maladaptive remodeling of the heart. *PLoS One* **8**, e73294.

Xu, J., Gong, N.L., Bodi, I., Aronow, B.J., Backx, P.H. and Molkentin, J.D. (2006). Myocyte enhancer factors 2A and 2C induce dilated cardiomyopathy in transgenic mice. *J Biol Chem* **281**, 9152-9162.

Zhu, L., Fang, N., Gao, P., Jin, X. and Wang, H. (2009). Differential expression of alpha-enolase in the normal and pathological cardiac growth. *Exp Mol Pathol* **87**, 27-31.

Figures

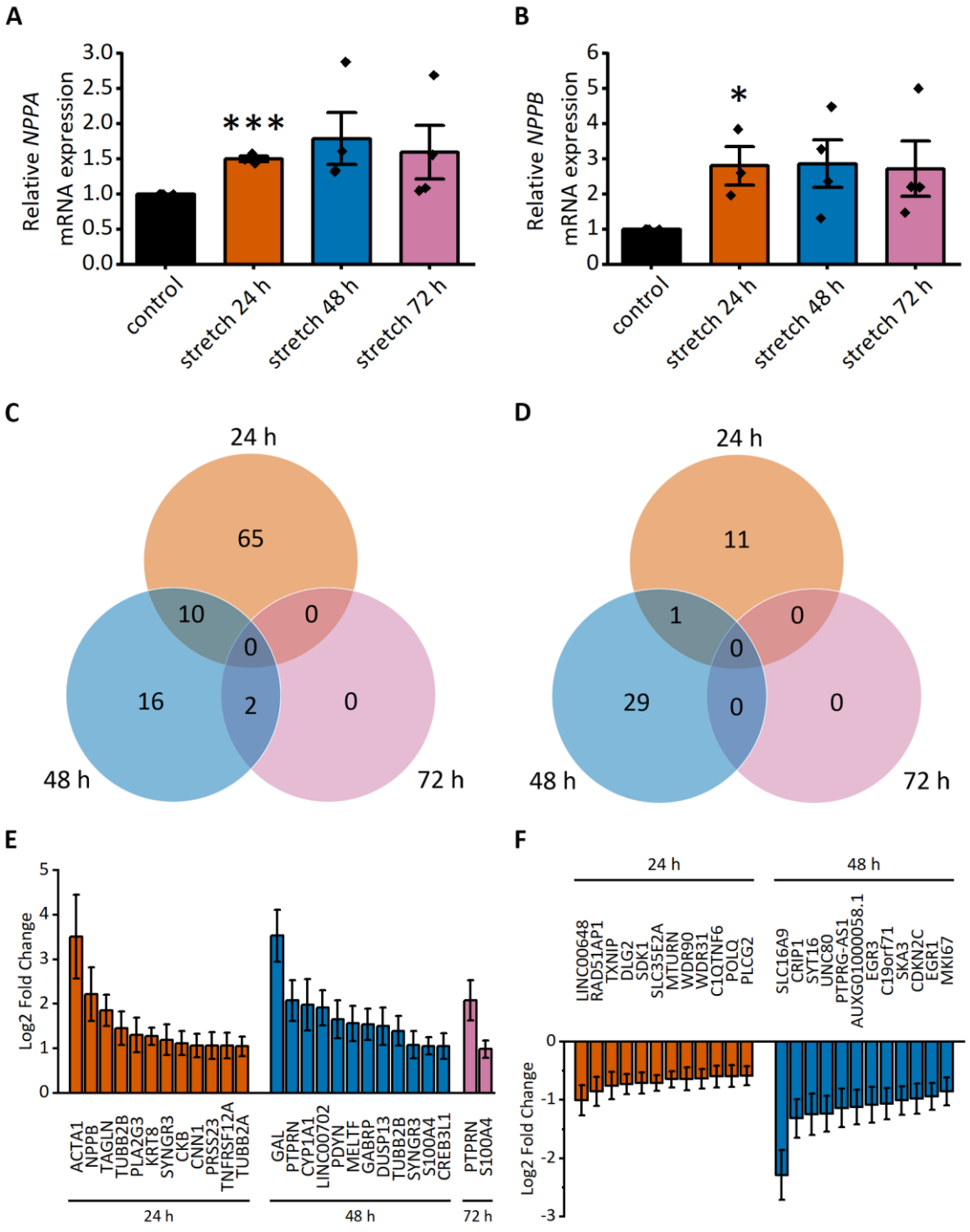

Figure 1. Mechanical stretch-induced differential gene expression of human induced pluripotent stem cell-derived cardiomyocytes (hiPSC-CMs). A-B, HiPSC-CMs respond to stretch by increased expression of hypertrophy-associated genes NPPA (natriuretic peptide A; A) and NPPB (natriuretic peptide B; B). mRNA expression of 24 h, 48 h and 72 h stretched hiPSC-CMs measured with qRT-PCR was normalized to the unstretched control. Bars present the mean, dots present individual values, and error bars present the standard error. *p<0.05, ***p<0.001 vs. unstretched control, Student's t-test

for independent samples. C-D, Venn diagrams show the number of upregulated (C) and downregulated (D) genes after 24 h, 48 h and 72 h of cyclic stretch measured with RNA sequencing. Differential expression was defined as a >1.5-fold change compared to the unstretched control. E-F, The expression of the top 12 up- (E) and downregulated (F) genes is presented as log2-fold change relative to the unstretched control ± standard error (n=3 for 24 h, n=4 for 48 h and 72 h, n represents biological replicates of cells from individual differentiations). Only statistically significant (Benjamini-Hochberg adjusted p<0.05) results are presented.

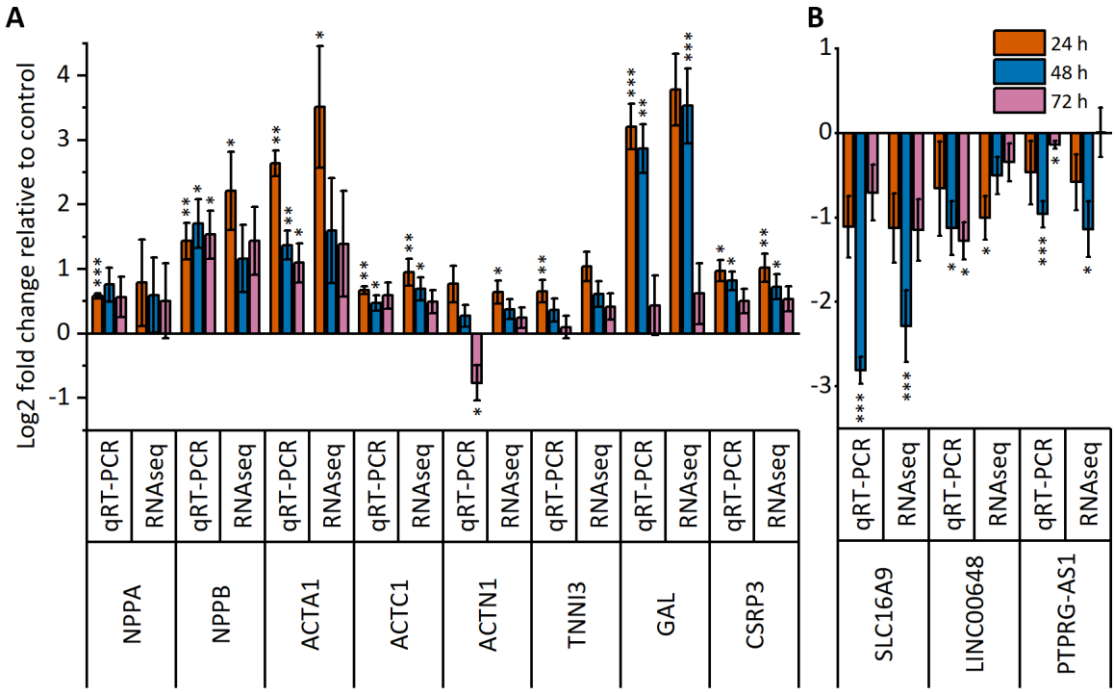

Figure 2. Time-dependent changes in gene expression of selected genes. Differential expression of 11 selected genes after 24 h, 48 h and 72 h of stretch was validated by qRT-PCR and RNA sequencing. The results are presented as log2-fold change relative to the unstretched control ± standard error (n=3 for 24 h, n=4 for 48 h and 72 h, n represents biological replicates of cells from individual differentiations) for upregulated (A) and downregulated (B) genes. *p<0.05, **p<0.01, ***p<0.001 vs. unstretched control, Student's t-test for independent samples (qRT–PCR), Wald test (RNAseq).

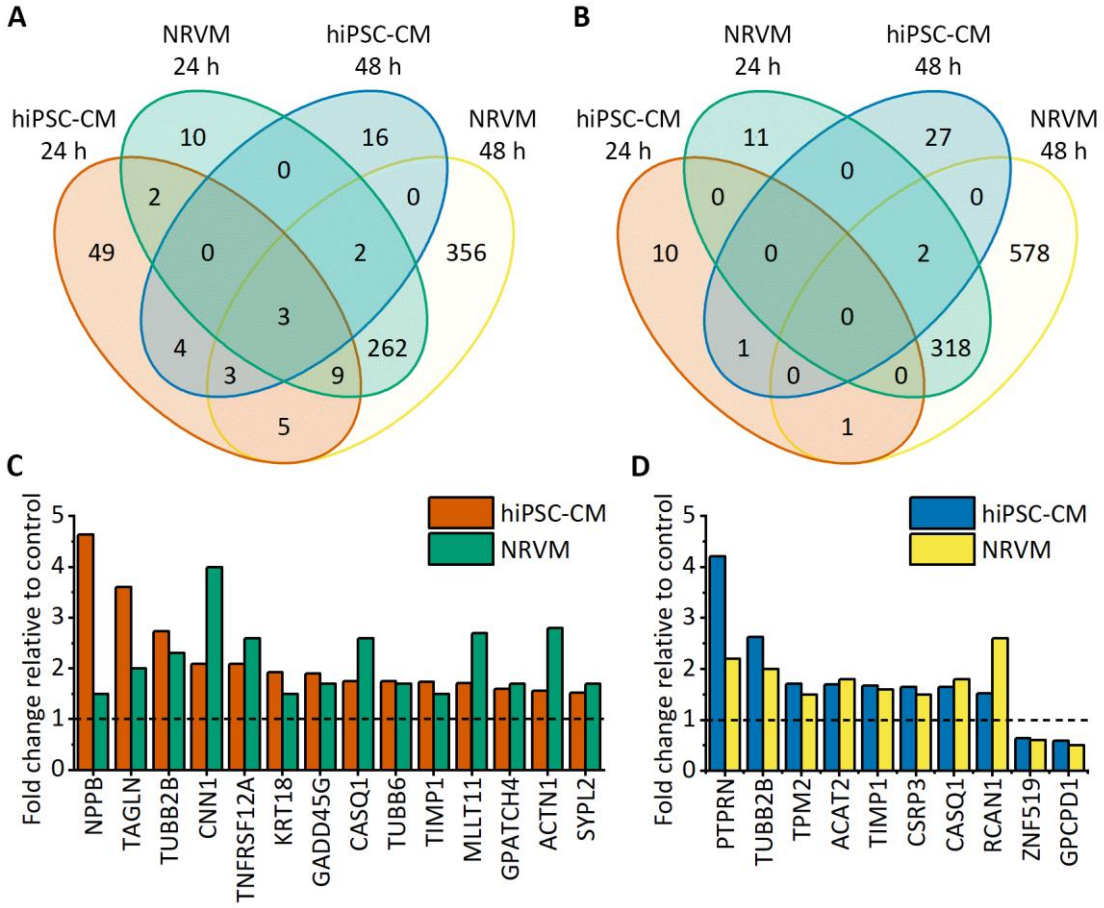

Figure 3. Comparison of differentially expressed genes in human induced pluripotent stem cell-derived cardiomyocytes (hiPSC-CMs) and neonatal rat ventricular myocytes (NRVMs) after 24 h and 48 h of stretch. NRVM gene expression data are from Rysä et al. (Rysä et al., 2018). A-B, Venn diagrams show the number of upregulated (A) and downregulated (B) genes after 24 h and 48 h of stretch in hiPSC-CMs and NRVMs. C-D, Expression of genes differentially regulated in both cell types after 24 h (C) and 48 h (D) of stretching normalized to the unstretched control (n=3 for 24 h hiPSC-CMs, n=4 for 48 h and 72 h hiPSC-CMs, and n=5 for NRVMs).

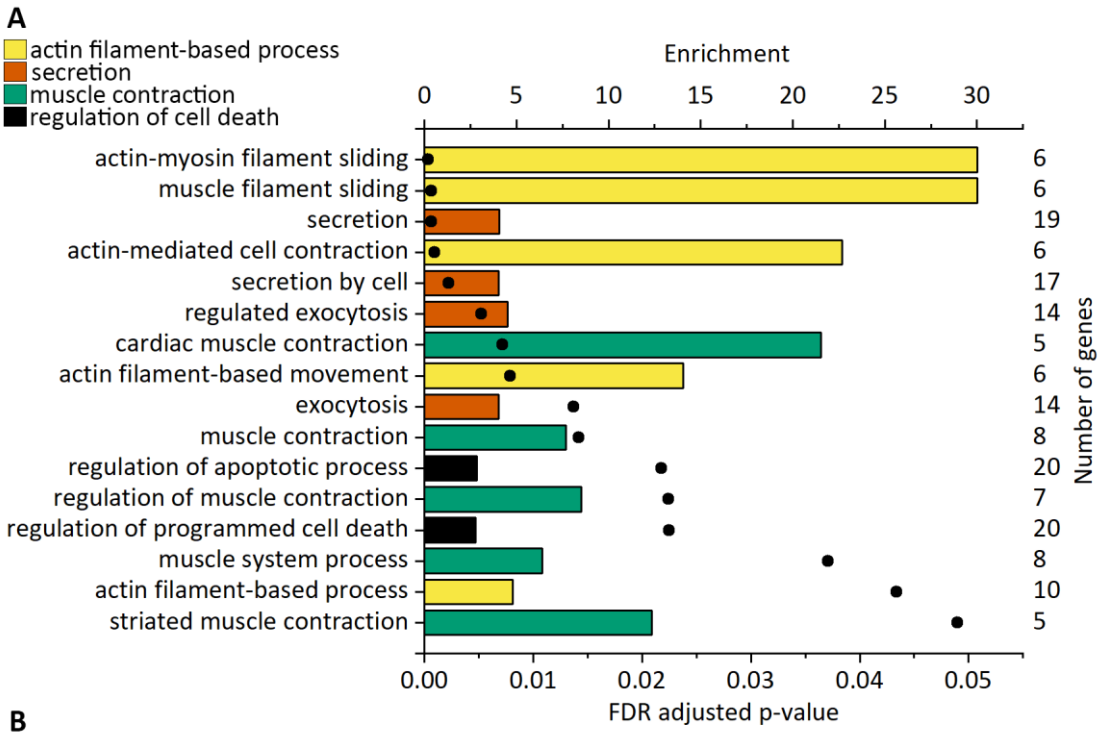

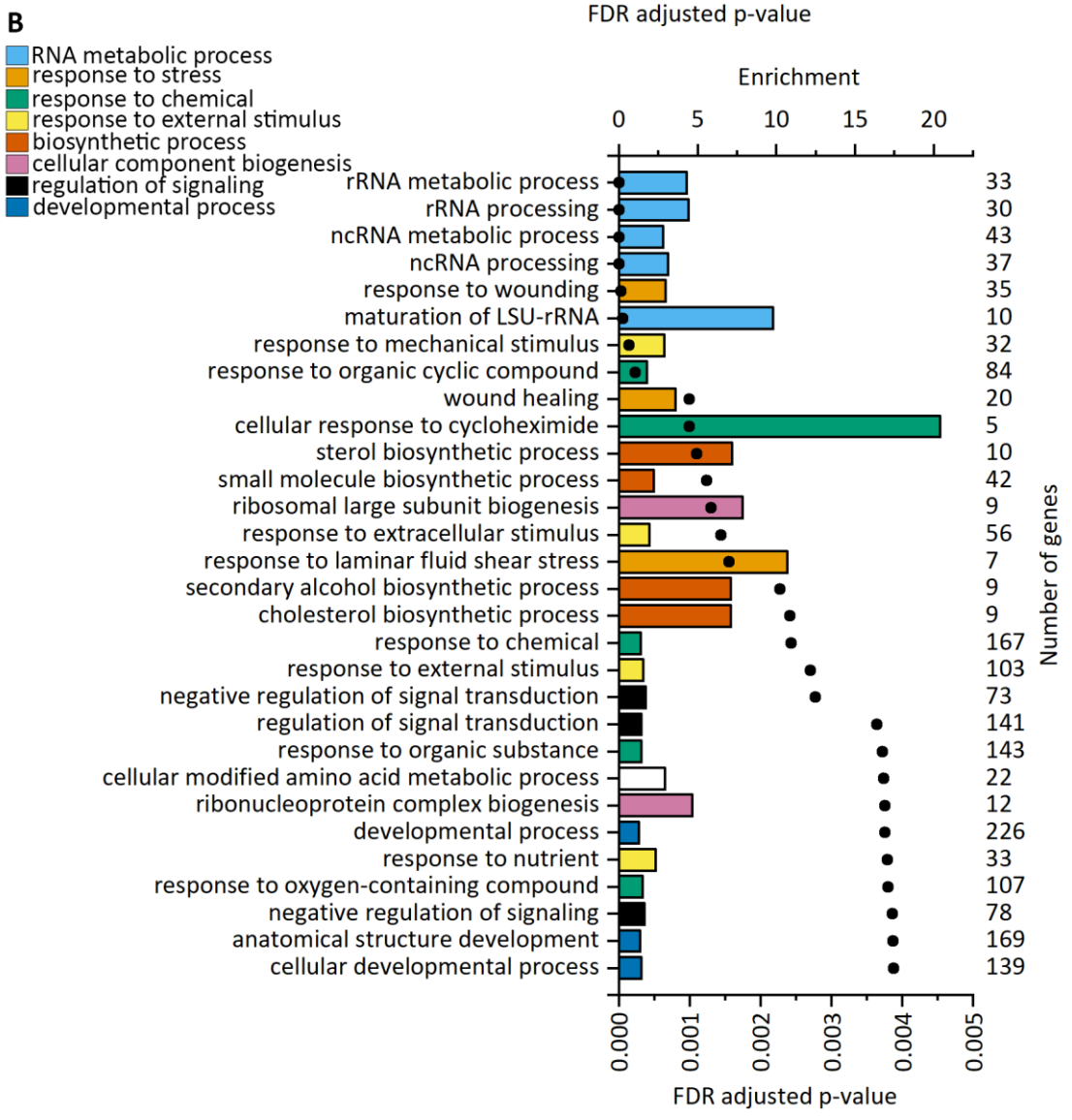

675 **Figure 4. Enriched biological processes in upregulated genes after cyclic stretch in human**
676 **induced pluripotent stem cell-derived cardiomyocytes (hiPSC-CMs; A) and neonatal rat**
677 **ventricular myocytes (NRVMs; B).** Gene Ontology (GO) enrichment analysis was performed with
678 GOrilla. For each significantly enriched GO term, enrichment values are presented as bars, and FDR-
679 adjusted p values are presented as dots. The number of upregulated genes associated with each GO
680 term is shown on the right. The upregulated genes in the NRVMs used for the analysis are from Rysä
681 et al. (Rysä et al., 2018). The top 30 terms for NRVMs are shown.

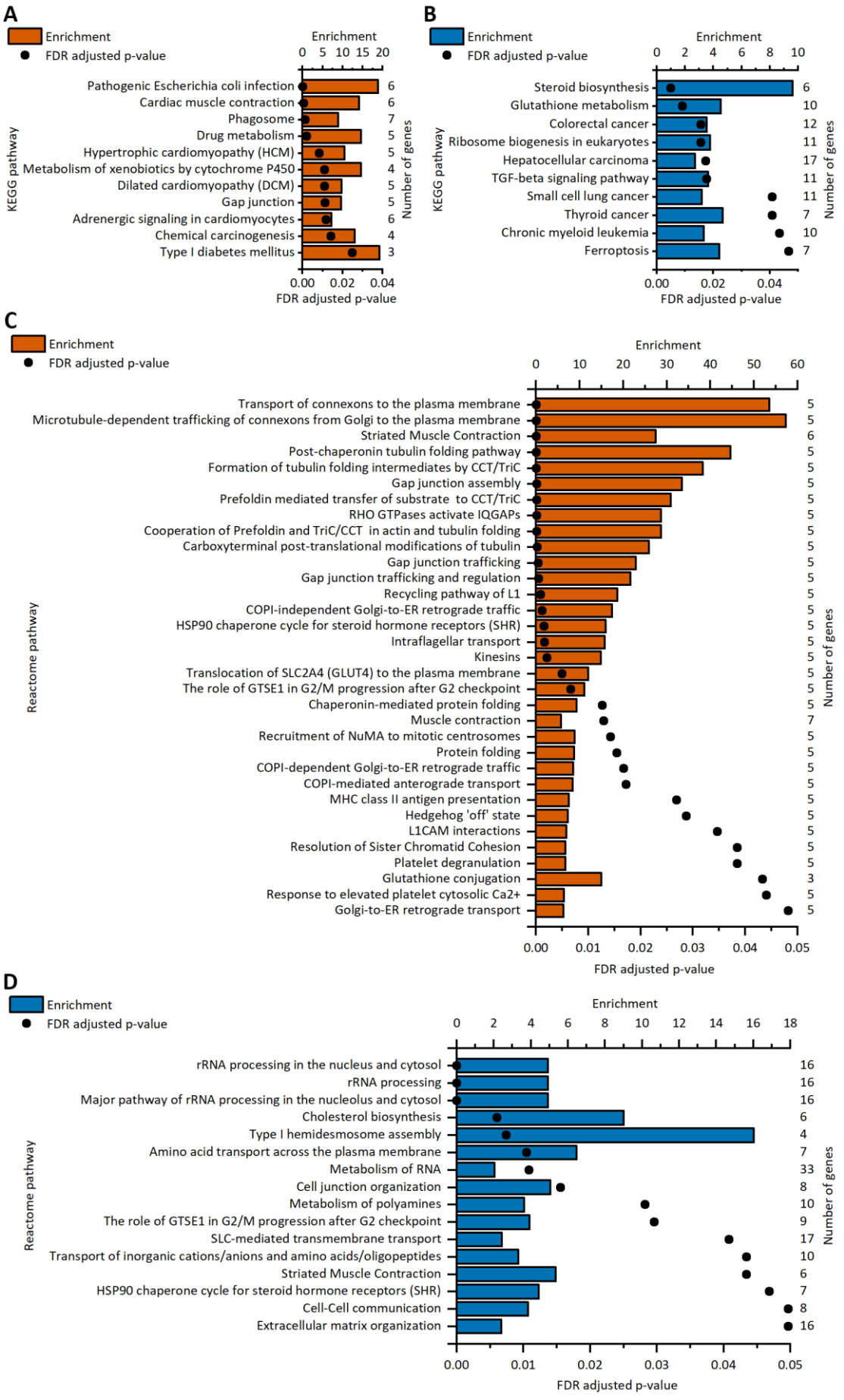

Figure 5. Enriched pathways in upregulated genes after cyclic stretch in human induced pluripotent stem cell-derived cardiomyocytes (hiPSC-CMs) and neonatal rat ventricular myocytes (NRVMs). A-B, KEGG pathway analyses of upregulated genes of stretched hiPSC-CMs (A) and NRVMs (B). C-D, Reactome pathway analyses of upregulated genes of stretched hiPSC-CMs (C) and NRVMs (D). For each significantly enriched pathway term, enrichment values are presented as bars, and FDR-adjusted p values are presented as dots. The number of upregulated genes associated with each term is shown on the right. The upregulated genes in the NRVMs used for the analysis are from Rysä et al. (Rysä et al., 2018).

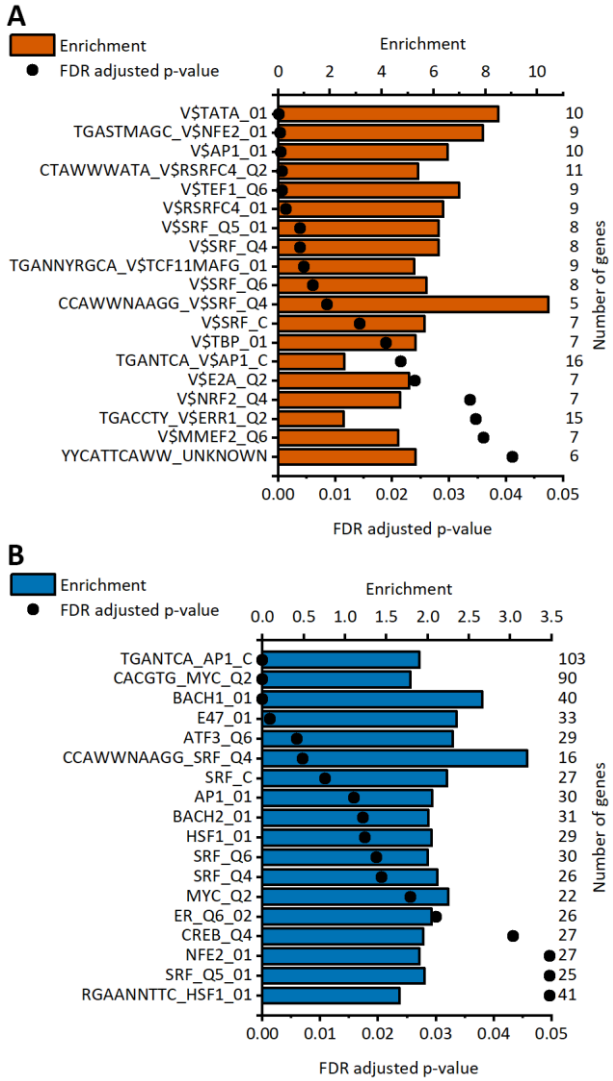

Figure 6. Enriched transcription factor target sites in the upregulated genes of the stretched human induced pluripotent stem cell-derived cardiomyocytes (hiPSC-CMs; A) and neonatal rat ventricular myocytes (NRVMs; B). Enrichment values for each significantly enriched target site are presented as bars, and FDR-adjusted p values are presented as dots. The number of upregulated genes associated with each target site is shown on the right. The upregulated genes in NRVMs used for the analysis are from Rysä et al. (Rysä et al., 2018).

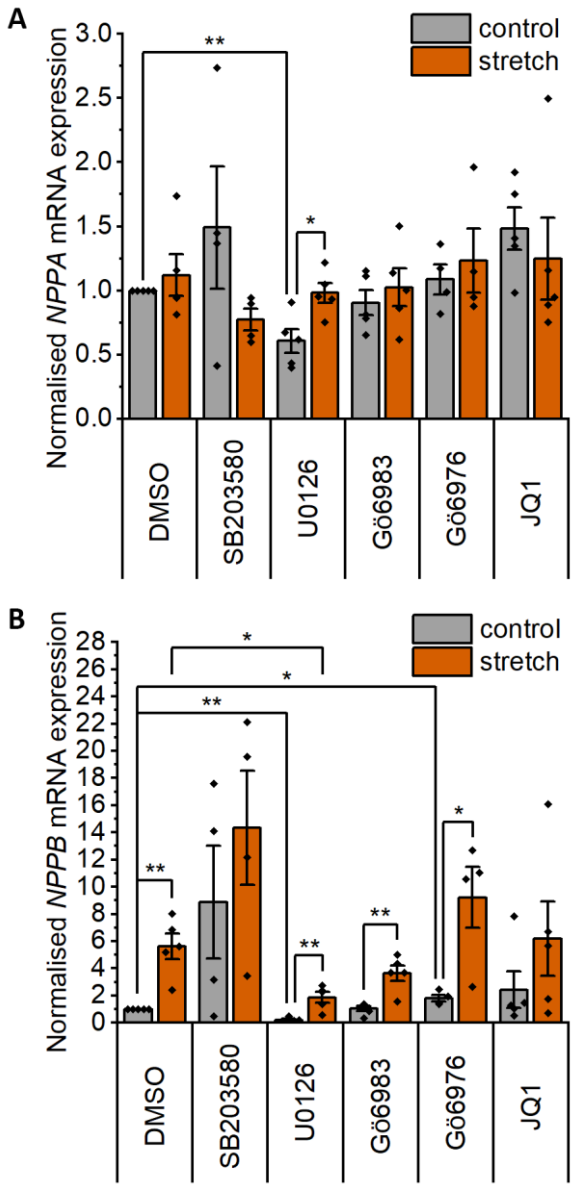

Figure 7. Effects of p38 mitogen-activated protein kinase (p38 MAPK), mitogen-activated protein kinase kinase 1/2 (MEK1/2), protein kinase C (PKC) and bromodomain and extraterminal domain (BET) inhibitors on stretch-induced hypertrophic gene expression. The following inhibitors were used: SB203580 at 10 µM to inhibit p38 MAPK, U0126 at 10 µM to inhibit MEK1/2, Gö6983 at 1 µM to inhibit all PKC isoforms, Gö6976 at 1 µM to inhibit classical PKC isoforms, and JQ1 at 300 nM to inhibit BET. Natriuretic peptide A (NPPA; A) and natriuretic peptide B (NPPB; B) mRNA expression was measured after cyclic mechanical stretch for 24 h with qRT–PCR, and the results are presented as the fold change relative to the unstretched control. Bars present the mean, dots present individual values, and error bars present the standard error of mean (n=5, except for SB203580 and Gö6976 n=4, n represents biological replicates of cells from individual differentiations). *p<0.05, **p<0.01, Mann–Whitney U test.